



## Intrafractional motion detection for spine SBRT via X-ray imaging using ExacTrac Dynamic

Johannes Muecke<sup>a,\*</sup>, Daniel Reitz<sup>a,e</sup>, Lili Huang<sup>a</sup>, Vanessa da Silva Mendes<sup>a</sup>,  
Guillaume Landry<sup>a</sup>, Michael Reiner<sup>a</sup>, Claus Belka<sup>a,b</sup>, Philipp Freislederer<sup>c</sup>,  
Stefanie Corradini<sup>a,1</sup>, Maximilian Niyazi<sup>a,d,1</sup>

<sup>a</sup> Department of Radiation Oncology, University Hospital, LMU Munich, Munich, Germany

<sup>b</sup> German Cancer Consortium (DKTK), Partner Site Munich, Munich, Germany

<sup>c</sup> Brainlab AG, Munich, Germany

<sup>d</sup> Department of Radiation Oncology, University Hospital Tübingen, Tübingen, Germany

<sup>e</sup> Strahlentherapie Nymphenburg/Fürstfeldbruck, Munich, Germany

### ARTICLE INFO

#### Keywords:

Spine stereotactic body radiotherapy  
Intrafraction motion detection  
X-ray stereoscopic imaging  
ExacTrac Dynamic  
Patient immobilization

### ABSTRACT

**Purpose:** Due to its close vicinity to critical structures, especially the spinal cord, standards for safety for spine stereotactic body radiotherapy (SBRT) should be high. This study was conducted, to evaluate intrafractional motion during spine SBRT for patients without individualized immobilization (e.g., vacuum cushions) using high accuracy patient monitoring via orthogonal X-ray imaging.

**Methods:** Intrafractional X-ray data were collected from 29 patients receiving 79 fractions of spine SBRT. No individualized immobilization devices were used during the treatment. Intrafractional motion was monitored using the ExacTrac Dynamic (ETD) System (Brainlab AG, Munich, Germany). Deviations were detected in six degrees of freedom (6 DOF). Tolerances for repositioning were 0.7 mm for translational and 0.5° for rotational deviations. Patients were repositioned when the tolerance levels were exceeded.

**Results:** Out of the 925 pairs of stereoscopic X-ray images examined, 138 (15 %) showed at least one deviation exceeding the predefined tolerance values. In all 6 DOF together, a total of 191 deviations out of tolerance were recorded. The frequency of deviations exceeding the tolerance levels varied among patients but occurred in all but one patient. Deviations out of tolerance could be seen in all 6 DOF. Maximum translational deviations were 2.6 mm, 2.3 mm and 2.8 mm in the lateral, longitudinal and vertical direction. Maximum rotational deviations were 1.8°, 2.6° and 1.6° for pitch, roll and yaw, respectively. Translational deviations were more frequent than rotational ones, and frequency and magnitude of deviations showed an inverse correlation.

**Conclusion:** Intrafractional motion detection and patient repositioning during spine SBRT using X-ray imaging via the ETD System can lead to improved safety during the application of high BED in critical locations. When using intrafractional imaging with low thresholds for re-positioning individualized immobilization devices (e.g. vacuum cushions) may be omitted.

**Abbreviations:** AP, anterior-posterior; BED, biologically effective dose; CI, confidence interval; CBCT, cone beam computed tomography; CT, computed tomography; CTV, clinical target volume; DOF, degrees of freedom; DRR, digitally reconstructed radiograph; ETD, ExacTrac Dynamic; GTV, gross tumor volume; kV, kilovolt; LINAC, linear accelerator; LR, left-right; MRI, magnetic resonance imaging; OAR, organ(s) at risk; PTV, planning target volume; SBRT, stereotactic body radiotherapy; SD, standard deviation; SEM, standard error of the mean; SGRT, surface guided radiotherapy; SI, superior-inferior; SIB, simultaneously integrated boost; SRS, stereotactic radiosurgery; VMAT, volumetric modulated arc therapy.

\* Corresponding authors at: Department of Radiation Oncology, University Hospital, LMU Munich, Marchioninstr. 15, 81377 Munich, Germany.

**E-mail addresses:** [johannes.muecke@med.uni-muenchen.de](mailto:johannes.muecke@med.uni-muenchen.de) (J. Muecke), [Lili.Huang@med.uni-muenchen.de](mailto:Lili.Huang@med.uni-muenchen.de) (L. Huang), [vanessa.mendes@med.uni-muenchen.de](mailto:vanessa.mendes@med.uni-muenchen.de) (V. da Silva Mendes), [guillaume.landry@med.uni-muenchen.de](mailto:guillaume.landry@med.uni-muenchen.de) (G. Landry), [philipp.freislederer@brainlab.com](mailto:philipp.freislederer@brainlab.com) (P. Freislederer), [stefanie.corradini@med.uni-muenchen.de](mailto:stefanie.corradini@med.uni-muenchen.de) (S. Corradini), [Maximilian.Niyazi@med.uni-tuebingen.de](mailto:Maximilian.Niyazi@med.uni-tuebingen.de) (M. Niyazi).

<sup>1</sup> Both authors contributed equally.

<https://doi.org/10.1016/j.ctro.2024.100765>

Received 21 July 2023; Received in revised form 13 March 2024; Accepted 14 March 2024

Available online 15 March 2024

2405-6308/© 2024 Published by Elsevier B.V. on behalf of European Society for Radiotherapy and Oncology. This is an open access article under the CC BY-NC-ND license (<http://creativecommons.org/licenses/by-nc-nd/4.0/>).

## 1. Introduction

Metastases to the spine are a common cause of morbidity in patients suffering from different types of cancer. Data indicate that spinal metastases might affect up to 70 % of metastatic cancer patients [1]. The standard treatment for these patients has traditionally been conventional palliative radiotherapy with a fractionation of 8 Gy in 1 fraction, 20 Gy in 5 fractions or 30 Gy in 10 fractions. However, conventional palliative radiotherapy is associated with poor local and poor long-term symptomatic control, with complete pain control rates of only 10–20 % [2–4]. In recent times, overall survival of patients with advanced tumor stages is improving due to technical advancements with improved diagnostics and improved and more individualized systemic treatment options. In this context, the term “oligometastatic disease” has been introduced to identify patients with limited metastatic disease who might benefit from additional and more aggressive local treatment regimens [5,6]. This is also true for patients with metastases to the spine. It was shown that patients with oligometastatic disease and spinal metastases have significantly better overall survival compared to patients with polymetastatic disease [7], indicating that these patients might also benefit from an ablative radiotherapy rather than from palliative treatment. Furthermore, recent data also indicate an improved pain control with the use of ablative versus conventional radiation doses [8]. Consequently, in recent years the development of stereotactic radiotherapy (SBRT) has been proven to be an established and effective therapeutic method for the treatment of spinal bone metastases [9–14]. This allows the application of a high biologically effective dose (BED) to the tumor tissue, leading to an improved local and symptomatic control compared to conventional radiotherapy.

Due to tight planning margins of only a 1–2 mm and steep dose gradients to the adjacent organs at risk (OAR), even minor deviations can lead to a geographic miss of the target or overdosage of critical neuronal structures, especially the spinal cord. With regard to the spinal cord, tolerances are well established, even in the case of re-irradiation [15]. Radiation myelopathy after spine SBRT is rare, but has been reported before and even in cases with unusually low doses, where technical errors might have been a problem [15,16]. Therefore, standards for safety for spine SBRT should be high. For the safe administration of SBRT, an advanced image guidance system and reliable patient immobilization are usually fundamental requirements. Immobilization is usually achieved by using individualized vacuum body fixation [17,18]. Patient setup and position verification on a conventional (C-arm) linear accelerator is usually achieved using cone beam computed tomography (CBCT) scans with the couch angle at 0° [17,19]. During the treatment itself the patient position is usually not standardly monitored. Furthermore, the time gap between CBCT and treatment delivery can lead to undetected displacements despite using immobilization [18]. Recent technological developments have facilitated intrafractional motion detection with immediate correction of the patient positioning during each session of radiotherapy, for example by using stereoscopic X-ray imaging in combination with a 6D robotic couch [20–22]. This may lead to safe administration of high dose radiotherapy in critical locations during long treatment durations and even with the omission of immobilization devices [23].

The aim of the present study was to assess intrafractional motion during spine SBRT via intrafractional X-ray imaging with the ExacTrac Dynamic (ETD) System (Brainlab AG, Munich, Germany) for patients without vacuum immobilization.

## 2. Material/methods

### 2.1. Patients and treatment planning

Intrafractional X-ray data were collected from patients receiving spine SBRT between November 2020 and August 2021 at the Department of Radiation Oncology, University Hospital, LMU Munich. For this,

patients were recruited in a prospective study and RT related information and patient characteristics were retrieved from medical records. Treatment was performed using a Versa HD (Elekta AB, Sweden) linear accelerator (LINAC) and image-guidance with the ETD System. Metastases were located in the thoracic and lumbar spine. Inclusion criteria for SBRT to the spine included a Karnofsky performance score  $\geq 50$  %, oligometastatic disease ( $\leq 5$  active tumor sites), a stable spine (SINS score  $\leq 6$ ) and no or little epidural involvement (Bilsky Score  $\leq 1$ ). The study was approved by the local ethics committee of the University Hospital, LMU Munich (No. 20-626 ex 08/2020). Written informed consent was obtained from all participants.

All patients underwent diagnostic (non-treatment position) volumetric magnetic resonance imaging (MRI) of the target region (T1-weighted with contrast enhancement and T2-weighted with 1.5–2 mm slice thickness) and computed tomography (CT) simulation (1-mm-slice thickness) for tumor delineation and treatment planning. CT and MRI image fusion and target delineation was done using the Brainlab Elements Spine SRS tool (Brainlab AG, Munich, Germany). This software calculates individual rigid image co-registrations for each vertebra and, thereafter, a single 3D deformation field that matches all vertebrae in the fused images at the same time is determined [24,25]. Target volume definition was performed according to the international spine radio-surgery consensus guidelines [26]. Typically, for the PTV a 2 mm margin was applied to the CTV with avoidance of the spinal canal. A 1.5 mm planning OAR volume (PRV) margin was applied to the spinal cord with the strictest constraint on the maximum dose to the PRV. Furthermore, we implemented a simultaneous integrated boost (SIB) concept including a boost to the GTV with 3 mm margin. All patient treatments were planned using the Monaco treatment planning system (Elekta AB, Sweden). Treatment was carried out with 2–4 (mode: 3) coplanar volumetric arc therapy (VMAT) fields. Photon energy was 6 MV with a maximum dose rate of 600 MU per minute. Fractionation schedules included 2x 9/12 Gy (PTV/SIB PTV), 3x 7/9 Gy and 5x 5/6 Gy with the maximum dose limited to 125 %.

### 2.2. ExacTrac Dynamic system

Intrafractional motion was detected via ETD, which uses a combination of X-ray imaging and a hybrid optical surface and thermal imaging scanner. The thermal camera acts as an additional registration information to the surface information, to increase the registration accuracy [27]. However, in this work only X-ray data were used to analyze intrafractional motion, since X-ray-based image-guidance by bone matching is a reliable and standard method for positioning in spine SBRT due to close proximity of OAR to bony spinal structures. The specifications for the x-ray imaging were as follows: 120 kV, 20 mAs, 3.53 mm aluminum filtration, 178.125 mm x 178.125 mm FOV at the isocentre.

### 2.3. Clinical workflow

For planning CT scan and treatment, patients were positioned in a supine position on the couch with the arms up or down at the sides depending on the treatment location and with an optional knee cushion for comfort. No patient-specific vacuum cushion immobilization devices were used.

All patients received VMAT treatment. After the initial surface guided positioning via ETD on the treatment couch, stereoscopic kilovolt (kV) X-ray images of the relevant bony structures of the spine were acquired by two detectors for sub-millimeter position corrections by comparison with digitally reconstructed radiographs (DRR). Deviations in six degrees of freedom (6 DOF) were obtained (3 translations: lateral, longitudinal, vertical; 3 rotations: roll, pitch, yaw) and subsequently sent to the robotic Hexapod couch (Elekta HexaPOD evo RT System with iGUIDE 2.2.x, Elekta AB, Sweden), which was able to precisely correct the position in all 6 DOF. Thereafter, another pair of stereoscopic X-ray images was taken to verify the corrected position. CBCT was not used for

the initial patient setup nor for the following patient monitoring during the treatment.

During the irradiation, intrafractional stereoscopic X-ray images were acquired for each treatment beam during beam on time at gantry positions 0°, 90°, 180° and 270°. For other gantry angles only monoscopic X-ray imaging is possible due to occlusion of the X-ray source or the detector by the gantry. This lead to a maximum of four sets of stereoscopic image pairs per arc and a mean of 12 X-ray image pairs per fraction. Based on the registration of these X-ray images to the previously generated DRRs, the system automatically detected target deviations along the 3 translational and 3 rotational axes. In case of a deviation larger than 0.7 mm for translational movement or 0.5° for rotational movement, the treatment beam was automatically held and the patient was re-positioned after manual review by a trained physician or radiation therapist. Fig. 1 shows a screenshot of the monitored ETD during irradiation.

#### 2.4. Data processing

X-ray-imaging-based deviation data in 6 DOF (lateral, longitudinal and vertical translational position deviations in millimeters; roll-, pitch- and yaw-angles for rotational deviations in degrees) were retrieved from PDF-file records that were generated for every treatment session of a patient and contain all the relevant measured datasets.

#### 2.5. Statistical analyses

The mean, standard error of the mean (SEM) and standard deviation (SD) were calculated for the different spatial axes. Since there was no exact normal distribution for the measured parameters, additional information including median values and 95 %-confidence intervals (CI) were provided to reliably describe the data distributions. MATLAB (R2020b, The MathWorks, Inc., Natick, Massachusetts, United States) was utilized for data extraction as well as data processing and GraphPad Prism (Version 7, GraphPad Software, San Diego, USA) for statistical analyses and visualization.

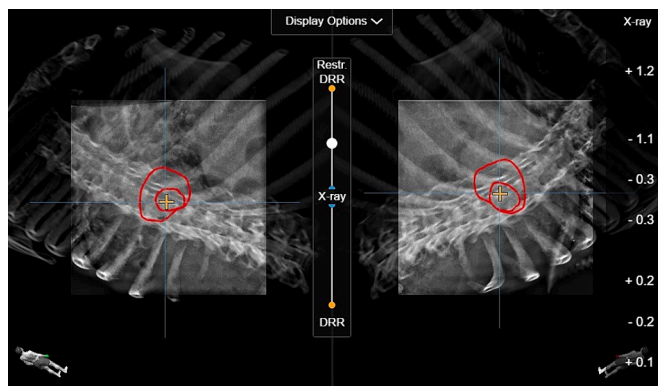


**Fig. 1.** Intrafractional motion detection using X-ray imaging. Stereoscopic X-ray images were acquired before and during spine SBRT and were instantly fused to the planned position to detect patient displacement. While preparing the plan in the ETD system, a volume of interest was defined by restricting the CT volume. Moreover, non-relevant areas were excluded to improve the accuracy of the fusion between the X-ray images and the DRRs. When out of tolerance, the user was alerted by the system and the patient position was corrected. Tolerance for intrafractional correction was 0.7 mm for translational deviations and 0.5° for rotational deviations. The red lines in the X-rays represent the planning target volume and simultaneously integrated boost area. (For interpretation of the references to colour in this figure legend, the reader is referred to the web version of this article.)

### 3. Results

#### 3.1. Patient and tumor/treatment characteristics

Treatment data were acquired from 21 patients and 79 fractions of spine SBRT. Metastases were located in the lumbar (38 %) and thoracic spine (62 %). 13 patients received SBRT in 5 fractions, 3 patients in 3 fractions and 5 patients in 2 fractions. Tumor entities varied, with the most common being prostate cancer, sarcoma and breast cancer. Further and more detailed patient and treatment characteristics are shown in Table 1.

#### 3.2. Descriptive analysis

After excluding error data (for example when only one of the two X-ray detectors could acquire X-ray data due to the LINAC position), 79 treatment fractions and 925 stereoscopic X-ray image pairs were analyzed. Overall, 138 image pairs (15 %) showed a deviation exceeding the tolerance levels in at least one DOF. In all 6 DOF together, a total of 191 deviations out of tolerance were recorded (of 925 x 6 = 5550 possible). Table 2 shows that deviations out of tolerance occurred among all patients but one. However, frequency of deviations out of tolerance varied, with some patients accounting for many deviations, while others only had few. Only one patient (a 61-year-old female with breast cancer who was treated with 2x 9/12 Gy to a metastasis in L2) had no deviation out of tolerance and thus did not need a re-positioning during radiotherapy. In 103 of the images pairs a deviation out of tolerance was detected in only one DOF, and in 35 image pairs there were deviations out of tolerance in two or more DOF. Only in one single X-ray image pair tolerances were exceeded in all 6 DOF. Mean absolute deviations were 0.31 mm, 0.30 mm and 0.19 mm in the lateral, longitudinal and vertical direction and 0.14°, 0.17° and 0.13° for pitch, roll and yaw, respectively. Most translational deviations out of tolerance occurred in the lateral axis (n = 59) and most rotational deviations out of tolerance in the roll axis (n = 29). Maximum translational deviations were 2.6 mm, 2.3 mm and 2.8 mm in the lateral, longitudinal and vertical direction. Maximum rotational deviations were 1.8°, 2.6° and 1.6° for pitch, roll and yaw, respectively. Translational deviations out of tolerance occurred more frequently (in 112/925 image pairs, 12.1 %) than rotational ones (in 49/925 image pairs, 5.2 %) and occurred most frequently in the lateral (n = 59) and longitudinal axis (n = 52). Yaw deviations exceeding tolerance were the least frequent (n = 9). The distribution of deviations was bi-directional in all six DOF and was centered around the origin (Fig. 2). Frequency distribution (Fig. 3) showed that most deviations were, as expected, close to the origin and

**Table 1**  
Patient, tumor and treatment characteristics.

| Variables                            | Number   |
|--------------------------------------|--|
| Number of patients                   | 21 (100 %)   |
| Age                                  | 73 (47–84)   |
| Gender                               | 15 (71 %)<br>male<br>6 (29 %)<br>female  |
| Tumor localisation                   | 13 (62 %)<br>thoracic spine<br>8 (38 %)<br>lumbar spine  |
| Tumor entity (primary histology)     | 9 (43 %)<br>prostate cancer<br>2 (10 %)<br>lung cancer<br>3 (14 %)<br>sarcoma<br>3 (14 %)<br>breast cancer<br>1 (5 %)<br>cholangiocellular carcinoma<br>2 (10 %)<br>colorectal cancer<br>1 (5 %)<br>thyroid cancer |
| Dose prescription (CTV/SIB GTV)      | 13 (62 %)<br>5x 5/6 Gy<br>3 (14 %)<br>3x 7/9 Gy<br>5 (24 %)<br>2x 9/12 Gy  |
| Total number of fractions evaluated  | 79   |
| Number of X-ray image pairs analyzed | 925  |

**Table 2**

Number and percentage of X-ray images exceeding the tolerance for each patient.

| Patient number | Number of X-ray image pairs with at least one deviation out of tolerance | Number of X-ray image pairs acquired | Percentage of X-ray image pairs with at least one deviation out of tolerance |
|----------------|--|--------------------------------------|--|
| 1              | 4  | 15                                   | 27 %   |
| 2              | 11   | 44                                   | 25 %   |
| 3              | 5  | 59                                   | 8 %  |
| 4              | 4  | 24                                   | 17 %   |
| 5              | 9  | 25                                   | 36 %   |
| 6              | 1  | 36                                   | 3 %  |
| 7              | 8  | 60                                   | 13 %   |
| 8              | 4  | 59                                   | 7 %  |
| 9              | 9  | 54                                   | 17 %   |
| 10             | 5  | 60                                   | 8 %  |
| 11             | 6  | 60                                   | 10 %   |
| 12             | 0  | 24                                   | 0 %  |
| 13             | 15   | 43                                   | 35 %   |
| 14             | 4  | 36                                   | 11 %   |
| 15             | 4  | 45                                   | 9 %  |
| 16             | 6  | 64                                   | 9 %  |
| 17             | 12   | 57                                   | 21 %   |
| 18             | 15   | 52                                   | 29 %   |
| 19             | 2  | 21                                   | 10 %   |
| 20             | 8  | 45                                   | 18 %   |
| 21             | 6  | 42                                   | 14 %   |
| All            | 138  | 925                                  | 15 %   |

frequency declined with deviation magnitude. Detailed statistics of absolute and relative deviations in all 6 DOF can be seen in Table 3.

**4. Discussion**

The present study analyzed intrafractional motion during spine SBRT without patient-specific immobilization using high accuracy patient monitoring via X-ray imaging (ETD system). ETD is an extension to ExacTrac X-ray, incorporating additional SGRT via optical and thermal scan of the patient surface [27,28]. The ExacTrac X-ray system is an established device for motion detection during spine SBRT [21,29] and is also commonly used for cranial stereotactic radiosurgery (SRS) [30,31]. In this work we focused on analyzing only the stereoscopic X-ray images acquired during the treatment and extracted from the ETD system. To continuously monitor the patient position, the optical and thermal information was also acquired throughout the whole treatment,

but with high thresholds to detect only large displacements between the X-ray images. We were able to show that the X-ray data extracted from the ETD system can be effectively used for intrafractional motion monitoring and for immediate correction of the body position, if necessary. This makes accurate and safe application of high BED in spine SBRT feasible, even without using individualized body immobilization devices.

If additional imaging is used, the question naturally arises as to whether this results in increased dose exposure to the patient in comparison to standard verification of the body position with CBCT. In this regard, the AAPM TG Report 75 reports some measurements that took place in the past with an older version of the ExacTrac system, as well as for the Elekta XVI kV CBCT [32]. For the ExacTrac system the measured entrance dose levels (for each pair of x-rays) were between 0.335 and 0.551 mGy. For the Elekta XVI kV CBCT, the measured doses at the centre and at the surface of a torso phantom were 16 and 23 mGy, respectively. More recently, VanNiekerk et al. have estimated the effective dose for an ExacTrac image pair to be at 0.05 mSv [22]. This is in the same order of magnitude and tends to be even less than the effective dose administered by CBCT, which others have reported on. For example, Kan et al. have estimated the effective doses to the body from standard mode CBCT for imaging of the head and neck, chest, and pelvis to be 10.3, 23.7, and 22.7 mSv per scan, respectively [33]. It is important to note that these values are only an approximation and should be used to put effective doses into perspective. We plan to evaluate this important topic in future follow-up studies. It should be noted that frequent intrafractional imaging should always be performed with the possible additional dose exposure in mind.

To our knowledge, we are the first reporting on intrafractional motion detection during spine SBRT using a conventional LINAC system without the use of individualized immobilization devices. Previous studies which have focused on investigating intrafractional motion usually refer to immobilized patients [19,34–36]. We found only one study reporting on intrafractional motion during spine SBRT without the use of individualized immobilization [23]. However, this study used the robotic S7 Cyberknife® system for treatment.

Our results clearly demonstrate the need for intrafractional tracking in spine SBRT. Due to steep dose gradients, even small shifts of the patient position during treatment can result in non-negligible dosimetric effects on critical structures, especially the spinal cord. Wang et al. reported that a 2 mm error in translational patient positioning in any direction can result in > 5 % loss of tumor coverage and > 25 % increase in maximum dose to the organs at risk [35]. We recorded translational

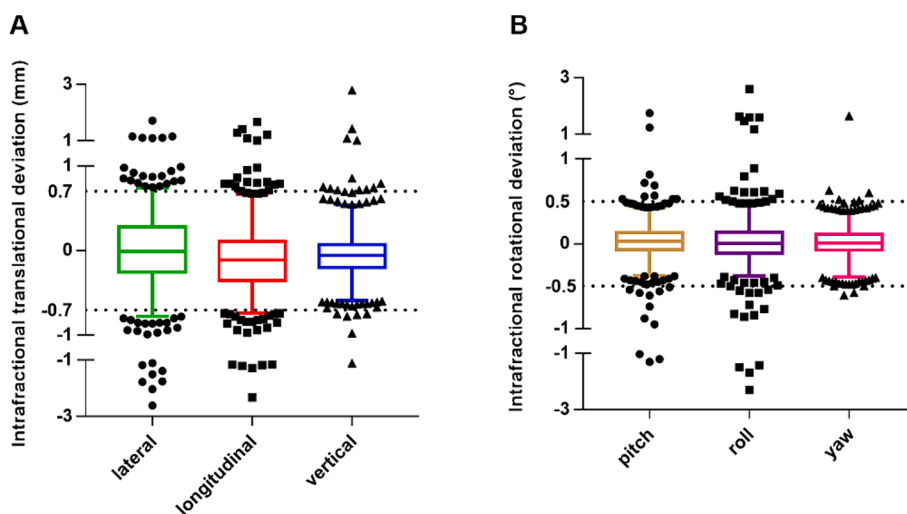


**Fig. 2.** The box plot shows a bi-directional distribution of intrafractional translational (A) and rotational (B) deviations during spine SBRT. Tolerances are shown as dotted lines and were 0.7 mm for translational and 0.5° for rotational deviations. Whiskers represent the 2.5 and 97.5 percentile. Values outside these percentiles are shown as symbols.



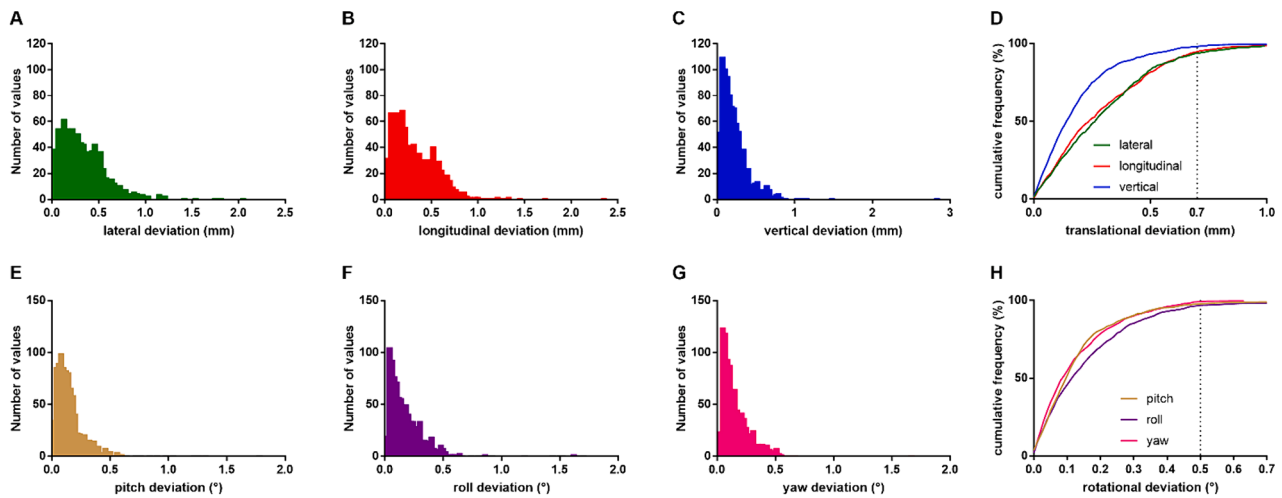


**Fig. 3.** A-C: Distribution of absolute translational deviations in all degrees of freedom (DOF); D: Cumulative frequency of translational deviation in all DOF (the black dotted line represents the threshold for re-positioning of the patient); E-F: Distribution of absolute rotational deviations in all DOF; H: Cumulative frequency of rotational deviation in all DOF (the black dotted line represents the threshold for re-positioning of the patient); n = 21 patients, 925 stereoscopic X-ray images.

**Table 3**  
Descriptive statistics for absolute and relative translational (left) and rotational (right) deviations during spine SBRT.

| Translational deviations        |            |             |          | Rotational deviations          |                         |              |             |            |            |
|---------------------------------|------------|-------------|----------|--------------------------------|-------------------------|--------------|-------------|------------|------------|
|                                 | lat<br>(x) | long<br>(y) | vert (z) | any                            |                         | pitch<br>(x) | roll<br>(y) | yaw<br>(z) | any        |
| n of values acquired            | 925        | 925         | 925      | 925                            | n                       | 925          | 925         | 925        | 925        |
| n over 0.5 mm                   | 163        | 177         | 64       | 329 (35.6 %)                   | n over tolerance (0.5°) | 21           | 32          | 9          | 49 (5.2 %) |
| n over tolerance<br>(0.7 mm)    | 59         | 52          | 18       | 112 (12.1 %)                   | n over 1°               | 5            | 10          | 1          | 12 (1.3 %) |
| n over 1 mm                     | 14         | 12          | 5        | 24 (2.6 %)                     |                         |              |             |            |            |
| n over 1.5 mm                   | 6          | 2           | 1        | 8 (0.9 %)                      |                         |              |             |            |            |
| <b>Absolute deviations (mm)</b> |            |             |          | <b>Absolute deviations (°)</b> |                         |              |             |            |            |
| Maximum                         | 2.60       | 2.32        | 2.79     |                                |                         | 1.75         | 2.60        | 1.64       |            |
| Median                          | 0.27       | 0.24        | 0.14     |                                |                         | 0.10         | 0.12        | 0.09       |            |
| Mean                            | 0.31       | 0.30        | 0.19     |                                |                         | 0.14         | 0.17        | 0.13       |            |
| Std. Deviation                  | 0.26       | 0.25        | 0.20     |                                |                         | 0.15         | 0.22        | 0.13       |            |
| Lower 95 % CI of mean           | 0.29       | 0.28        | 0.18     |                                |                         | 0.13         | 0.16        | 0.12       |            |
| Upper 95 % CI of mean           | 0.33       | 0.31        | 0.21     |                                |                         | 0.15         | 0.19        | 0.14       |            |
| <b>Relative deviations (mm)</b> |            |             |          | <b>Relative deviations (°)</b> |                         |              |             |            |            |
| Median                          | -0.01      | -0.11       | -0.06    |                                |                         | 0.03         | 0.00        | 0.01       |            |
| Mean                            | 0.00       | -0.10       | -0.05    |                                |                         | 0.03         | 0.02        | 0.01       |            |
| Std. Deviation                  | 0.41       | 0.37        | 0.27     |                                |                         | 0.20         | 0.28        | 0.18       |            |
| Lower 95 % CI of mean           | -0.03      | -0.13       | -0.07    |                                |                         | 0.02         | 0.00        | 0.00       |            |
| Upper 95 % CI of mean           | 0.03       | -0.08       | -0.04    |                                |                         | 0.04         | 0.03        | 0.02       |            |

lat: lateral; long: longitudinal; vert: vertical; 95 % CI: 95 % confidence interval.

deviations of 0.5 mm or more in 35.6 % of the radiographs and deviations out of tolerance (0.7 mm) in 12.1 % of the radiographs. Rotational deviations out of tolerance (0.5°) were less frequent with 5.2 %, yet far outliers (i.e., rotation over 1.5° occurred in 0.8 %) justify the registration and correction of rotational deviations, too. Rotational correction seems especially important for patients with multiple targets and for the setup of paraspinal targets when the isocenter is away from bony structures [35]. In total, 15 % of the 925 intrafractional radiographs showed out-of-tolerance deviations.

While maximum detected deviations were less than 3 mm for translations and less than 3° for rotations and larger deviations greater than 1.5 mm or over 1° occurred in only 0.9 % and 1.3 % of the X-ray image pairs respectively, this might be due to the high frequency of monitoring and the repeated correction of larger deviations throughout

the whole treatment time. This would be in agreement with Rossi et al., who used an intrafractional tracking approach during Cyberknife SBRT for non-immobilized patients similar to ours and analyzed patient displacement throughout the treatment time, quantifying displacements in comparison to time zero without taking into account intrafractional re-positionings. They showed that for non-immobilized patients the probability and magnitude of deviations increase with treatment delivery duration. For treatment times below 10 min they detected displacements > 2 mm in less than 2 %, while for longer treatment times over 30 min frequency increased to around 13 % [23]. Because the total treatment time is usually longer than 10 min for spine SBRT, intrafractional tracking should become a mandatory part of the treatment in case of omission of individualized immobilization.

Our results indicate that the omission of individualized

immobilization devices (e.g. vacuum mattresses) during spine SBRT is feasible when using intrafractional X-ray tracking and body repositioning. The deviations that we recorded during treatment along each direction were as follows (mean  $\pm$  SD): left–right (LR)  $0.31 \pm 0.26$  mm, superior–inferior (SI)  $0.30 \pm 0.25$  mm, and anterior–posterior (AP)  $0.19 \pm 0.20$  mm. This is less than the intrafractional motion that other studies have reported in immobilized patients (i.e., immobilization with vacuum mattresses or BodyFIX). For example, Yamoah et al. evaluated mid- and post-treatment errors using a stereotactic X-ray verification system in immobilized patients [29]. Patients were treated in all parts of the spine. Immobilization with the BodyFIX system (Elekta) was used for patients treated in the lower thoracic or lumbar spine. One mid-treatment verification X-ray image set as well as one post-treatment X-ray image set were acquired to determine deviations. The average translational errors mid-treatment for patients treated in the lower thoracic or lumbar spine were  $0.41 \pm 0.3$  mm (RL),  $0.41 \pm 0.3$  mm (SI) and  $0.45 \pm 0.3$  mm (AP). Finnigan et al. reported on intra-fraction motion during spine SBRT using a mid-treatment CBCT [17]. Lower thoracic and lumbosacral lesions were immobilized using a customized vacuum bag, thoracic wedge and knee bolster or subsequently using the BodyFIX system. Mean intra-fraction motion ( $\pm$ SD) was  $0.7$  mm ( $\pm 0.4$ ),  $0.6$  mm ( $\pm 0.5$ ) and  $0.6$  mm ( $\pm 0.5$ ) in x, y and z translational planes respectively; and  $0.4^\circ$  ( $\pm 0.4$ ),  $0.4^\circ$  ( $\pm 0.3$ ) and  $0.3^\circ$  ( $\pm 0.3$ ) in x, y and z rotational axes, respectively. Patients were treated in all parts of the spine. However, most tumors were located in the thoracic or lumbar spine and the authors found no statistically significant association between errors and tumor location. Svestad et al. assessed intrafraction motion in spine SBRT via post-treatment CBCT [37]. Tumor location was in the thoracic, lumbar and sacral spine. Patients were immobilized in an evacuated cushion (BlueBAG; Elekta). Two different cohorts were analyzed: one with an extra pre-treatment verification CBCT after the initial correction and one without. Mean post-treatment translational errors in the group without an extra verification CBCT were  $0.6 \pm 0.7$  mm (lateral),  $0.7 \pm 0.7$  mm (longitudinal) and  $0.5 \pm 0.6$  mm (vertical). An extra pre-treatment verification CBCT led to significantly less post-treatment deviations. All the above data indicate that the omission of immobilization during spine SBRT is applicable with the use of frequent X-ray tracking during the treatment. Frequent intrafractional motion detection for non-immobilized patients and subsequent body repositioning in case of larger body shifts leads to comparable or even better results in comparison to immobilized patients who are not being tracked during the treatment.

A main advantage of the present study is the automated gating function of the ETD system. If the deviation in any of the 6 DOF exceeds a prescribed tolerance range, the irradiation is stopped automatically without the need of any manual intervention. This leads to a fast and effective work flow. While deviations exceeding the tolerance occurred only in approximately 15 % of all X-ray images in our data set, there was a wide spread between patients (0–36 %), which shows that some patients benefit more than others from frequent motion detection. A limitation of our study is that we did not examine which factors influenced the magnitude and frequency of body motion (for example treatment time, tumor location, pain, etc.). This should be subject to further studies. Another limitation of the present study is that the sample rate is not as high as for example in surface guided radiotherapy, since X-ray images are acquired only at certain gantry positions and possible outliers could remain unobserved during this short amount of time between imaging.

## 5. Conclusion

The use of the ETD system facilitates the safe administration of spine SBRT in non-immobilized patients via X-ray based intrafractional motion detection. Most of the deviations we recorded via stereoscopic X-ray imaging were small and below the threshold for repositioning. Due to the frequent monitoring during treatment, larger deviations could be

detected and corrected within seconds. Omission of immobilization devices can lead to increased patient comfort during long treatment times when high radiation doses are delivered to complex target volumes.

## 6. Ethics approval and consent to participate

The study was approved by the local ethics committee of the University Hospital, LMU Munich (No. 20–626 ex 08/2020). Written informed consent was obtained from all participants.

## Funding

Funding for research with Brainlab ExacTrac Dynamic has been received from Brainlab AG. Brainlab AG was not involved and had no influence on the study design, the collection, analysis or interpretation of data, on the writing of the manuscript or the decision to submit the manuscript for publication.

## Authors' contributions

PF and VM performed data extraction. JM performed data processing, statistical analysis and drafted the manuscript. PF, VM, DR, GL, MR, MN, CB, SC reviewed the manuscript. MN helped to finalize the manuscript. PF and MR planned and organized the technical settings. CB and MN designed and supervised the study. All authors read and approved the final manuscript.

## Declaration of Competing Interest

The Department of Radiation Oncology, University Hospital, LMU Munich, Germany, received grants from Brainlab AG.

SC and MN received speaker fees and travel support from Brainlab AG.

PF is currently employed by Brainlab AG. However, at the time of the conception and draft of this manuscript, PF was not employed by Brainlab AG. PF declares that his employment had no influence on the design, the collection and the analysis of data, on the writing of the manuscript or the decision to submit the manuscript for publication.

## References

- [1] Sutcliffe P, Connock M, Shyangdan D, Court R, Kandala NB, Clarke A. A systematic review of evidence on malignant spinal metastases: natural history and technologies for identifying patients at high risk of vertebral fracture and spinal cord compression. *Health Technol Assess (rockv)* 2013;17(42). <https://doi.org/10.3310/hta17420>.
- [2] Foro Arnalot P, Fontanals AV, Galcerán JC, et al. Randomized clinical trial with two palliative radiotherapy regimens in painful bone metastases: 30 Gy in 10 fractions compared with 8 Gy in single fraction. *Radiother Oncol* 2008;89(2): 150–5. <https://doi.org/10.1016/j.radonc.2008.05.018>.
- [3] Nguyen J, Chow E, Zeng L, et al. Palliative response and functional interference outcomes using the brief pain inventory for spinal bony metastases treated with conventional radiotherapy. *Clin Oncol* 2011;23(7):485–91. <https://doi.org/10.1016/j.clon.2011.01.507>.
- [4] Sprave T, Verma V, Förster R, et al. Randomized phase II trial evaluating pain response in patients with spinal metastases following stereotactic body radiotherapy versus three-dimensional conformal radiotherapy. *Radiother Oncol* 2018;128(2):274–82. <https://doi.org/10.1016/j.radonc.2018.04.030>.
- [5] Hellman S, Weichselbaum RR. Oligometastases. *J Clin Oncol* 1995;13(1):8–10. <https://doi.org/10.1200/JCO.1995.13.1.8>.
- [6] Guckenberger M, Lievens Y, Bouma AB, et al. Characterisation and classification of oligometastatic disease: a European Society for Radiotherapy and Oncology and European Organisation for Research and Treatment of Cancer consensus recommendation. *Lancet Oncol* 2020;21(1):e18–28. [https://doi.org/10.1016/S1470-2045\(19\)30718-1](https://doi.org/10.1016/S1470-2045(19)30718-1).
- [7] Barzilai O, Versteeg AL, Sahgal A, et al. Survival, local control, and health-related quality of life in patients with oligometastatic and polymetastatic spinal tumors: a multicenter, international study. *Cancer* 2019;125(5):770–8. <https://doi.org/10.1002/cncr.31870>.
- [8] Sahgal A, Myrehaug SD, Siva S, et al. Stereotactic body radiotherapy versus conventional external beam radiotherapy in patients with painful spinal metastases: an open-label, multicentre, randomised, controlled, phase 2/3 trial.

- Lancet Oncol 2021;22(7):1023–33. [https://doi.org/10.1016/S1470-2045\(21\)00196-0](https://doi.org/10.1016/S1470-2045(21)00196-0).
- [9] Gerszten PC, Burton SA, Ozhasoglu C, Welch WC. Radiosurgery for spinal metastases: Clinical experience in 500 cases from a single institution. *Spine (Phila Pa 1976)* 2007;32(2):193-1910.1097/01.brs.0000251863.76595.a2.
- [10] Yamada Y, Bilsky MH, Lovelock DM, et al. High-dose, single-fraction image-guided intensity-modulated radiotherapy for metastatic spinal lesions. *Int J Radiat Oncol Biol Phys* 2008;71(2):484–90. <https://doi.org/10.1016/j.ijrobp.2007.11.046>.
- [11] Ahmed KA, Stauder MC, Miller RC, et al. Stereotactic body radiation therapy in spinal metastases. *Int J Radiat Oncol Biol Phys* 2012;82(5):e803–9. <https://doi.org/10.1016/j.ijrobp.2011.11.036>.
- [12] Tseng CL, Soliman H, Myrehaug S, et al. Imaging-based outcomes for 24 Gy in 2 daily fractions for patients with de novo spinal metastases treated with spine stereotactic body radiation therapy (SBRT). *Int J Radiat Oncol Biol Phys* 2018;102(3):499–507. <https://doi.org/10.1016/j.ijrobp.2018.06.047>.
- [13] Guckenberger M, Mantel F, Gerszten PC, et al. Safety and efficacy of stereotactic body radiotherapy as primary treatment for vertebral metastases: a multi-institutional analysis. *Radiat Oncol* 2014;9:226. <https://doi.org/10.1186/s13014-014-0226-2>.
- [14] Chang UK, Cho WI, Kim MS, Cho CK, Lee DH, Rhee CH. Local tumor control after retreatment of spinal metastasis using stereotactic body radiotherapy; Comparison with initial treatment group. *Acta Oncol (madr)* 2012;51(5):589–95. <https://doi.org/10.3109/0284186X.2012.666637>.
- [15] Sahgal A, Chang JH, Ma L, et al. Spinal cord dose tolerance to stereotactic body radiation therapy. *Int J Radiat Oncol Biol Phys* 2021;110(1):124–36. <https://doi.org/10.1016/j.ijrobp.2019.09.038>.
- [16] Katsoulakis E, Jackson A, Cox B, Lovelock M, Yamada Y. A detailed dosimetric analysis of spinal cord tolerance in high-dose spine radiosurgery. *Int J Radiat Oncol Biol Phys* 2017;99(3):598–607. <https://doi.org/10.1016/j.ijrobp.2017.05.053>.
- [17] Finnigan R, Lamprecht B, Barry T, et al. Inter- and intra-fraction motion in stereotactic body radiotherapy for spinal and paraspinal tumours using cone-beam CT and positional correction in six degrees of freedom. *J Med Imaging Radiat Oncol* 2016;60(1):112–8. <https://doi.org/10.1111/1754-9485.12353>.
- [18] Li W, Sahgal A, Foote M, Millar BA, Jaffray DA, Letourneau D. Impact of immobilization on intrafraction motion for spine stereotactic body radiotherapy using cone beam computed tomography. *Int J Radiat Oncol Biol Phys* 2012;84(2):520–6. <https://doi.org/10.1016/j.ijrobp.2011.12.039>.
- [19] Hyde D, Lochray F, Korol R, et al. Spine stereotactic body radiotherapy utilizing cone-beam CT image-guidance with a robotic couch: Intrafraction motion analysis accounting for all six degrees of freedom. *Int J Radiat Oncol Biol Phys* 2012;82(3):e555–62. <https://doi.org/10.1016/j.ijrobp.2011.06.1980>.
- [20] Chang Z, Wang Z, Ma J, O'Daniel JC, Kirkpatrick J, Yin FF. 6D image guidance for spinal non-invasive stereotactic body radiation therapy: Comparison between ExacTrac X-ray 6D with kilo-voltage cone-beam CT. *Radiat Oncol* 2010;95(1):116–21. <https://doi.org/10.1016/j.radonc.2009.12.036>.
- [21] Wu J, Wu J, Ballangrud Å, Mechalakos J, Yamada J, Lovelock DM. Frequency of large intrafractional target motions during spine stereotactic body radiation therapy. *Pract Radiat Oncol* 2020;10(1):e45–9. <https://doi.org/10.1016/j.prro.2019.08.006>.
- [22] vanNiekirk WM, Lazeroms T, Rogers SJ, et al. Optimized workflow to minimize intra-fractional motion during stereotactic body radiotherapy of spinal metastases. *Tech Innov Patient Support Radiat Oncol* 2022;24(September):40–7. <https://doi.org/10.1016/j.tipsro.2022.09.007>.
- [23] Rossi E, Fiorino C, Fodor A, et al. Residual intra-fraction error in robotic spinal stereotactic body radiotherapy without immobilization devices. *Phys Imaging Radiat Oncol* 2020;16(June):20–5. <https://doi.org/10.1016/j.phro.2020.09.006>.
- [24] Rashad A, Heiland M, Hiepe P, et al. Evaluation of a novel elastic registration algorithm for spinal imaging data: a pilot clinical study. *Int J Med Robot* 2019;15(3):e1991.
- [25] Rogé M, Henni AH, Neggaz YA, et al. Evaluation of a dedicated Software “ElementsTM spine SRS, brainlab®” for Target volume definition in the treatment of spinal bone metastases with stereotactic body radiotherapy. *Front Oncol* 2022;12(May):1–8. <https://doi.org/10.3389/fonc.2022.827195>.
- [26] Cox BW, Spratt DE, Lovelock M, et al. International spine radiosurgery consortium consensus guidelines for target volume definition in spine stereotactic radiosurgery. *Int J Radiat Oncol Biol Phys* 2012;83(5):e597–605. <https://doi.org/10.1016/j.ijrobp.2012.03.009>.
- [27] Freisleder P, Kügeler M, Öllers M, et al. Recent advanced in Surface guided radiation therapy. *Radiat Oncol* 2020;15(1):1–11. <https://doi.org/10.1186/s13014-020-01629-w>.
- [28] Da Silva MV, Reiner M, Huang L, et al. ExacTrac dynamic workflow evaluation: combined surface optical/thermal imaging and X-ray positioning. *J Appl Clin Med Phys* 2022;23(10):1–16. <https://doi.org/10.1002/acm2.13754>.
- [29] Yamoah K, Zaorsky NG, Siglin J, et al. Spine stereotactic body radiation therapy residual setup errors and intra-fraction motion using the stereotactic X-ray image guidance verification system. *Int J Med Physics, Clin Eng Radiat Oncol* 2014;03(01):1–8. <https://doi.org/10.4236/ijmpcero.2014.31001>.
- [30] Jin JY, Yin FF, Tenn SE, Medin PM, Solberg TD. Use of the BrainLAB ExacTrac X-ray 6D system in image-guided radiotherapy. *Med Dosim* 2008;33(2):124–34. <https://doi.org/10.1016/j.meddos.2008.02.005>.
- [31] Reitz D, Muecke J, da Silva MV, et al. Intrafractional monitoring of patients using four different immobilization mask systems for cranial radiotherapy. *Phys Imaging Radiat Oncol* 2022;23(July):134–9. <https://doi.org/10.1016/j.phro.2022.07.002>.
- [32] Murphy MJ, Balter J, Balter S, et al. The management of imaging dose during image-guided radiotherapy: report of the AAPM task group 75. *Med Phys* 2007;34(10):4041–63. <https://doi.org/10.1118/1.2775667>.
- [33] Kan MWK, Leung LHT, Wong W, Lam N. Radiation dose from cone beam computed tomography for image-guided radiation therapy. *Int J Radiat Oncol Biol Phys* 2008;70(1):272–9. <https://doi.org/10.1016/j.ijrobp.2007.08.062>.
- [34] Jin JY, Ryu S, Rock J, et al. Evaluation of residual patient position variation for spinal radiosurgery using the novalis image guided system. *Med Phys* 2008;35(3):1087–93. <https://doi.org/10.1118/1.2839097>.
- [35] Wang H, Shiu A, Wang C, et al. Dosimetric effect of translational and rotational errors for patients undergoing image-guided stereotactic body radiotherapy for spinal metastases. *Int J Radiat Oncol Biol Phys* 2008;71(4):1261–71. <https://doi.org/10.1016/j.ijrobp.2008.02.074>.
- [36] Ma L, Sahgal A, Hossain S, et al. Nonrandom Intrafraction Target motions and general strategy for correction of spine stereotactic body radiotherapy. *Int J Radiat Oncol Biol Phys* 2009;75(4):1261–5. <https://doi.org/10.1016/j.ijrobp.2009.04.027>.
- [37] Graadal Svestad J, Ramberg C, Skar B, Paulsen HT. Intrafractional motion in stereotactic body radiotherapy of spinal metastases utilizing cone beam computed tomography image guidance. *Phys Imaging Radiat Oncol* 2019;12(0424):1–6. <https://doi.org/10.1016/j.phro.2019.10.001>.